Translational–rotational coupling in supercooled liquids: Heterodyne detected density induced molecular alignment

G. Hinze, R. S. Francis, and M. D. Fayer[a)]
Department of Chemistry, Stanford University, Stanford, California 94305

(Received 9 April 1999; accepted 7 May 1999)

We present a new time domain technique for studying molecular orientational relaxation in viscous liquids. A molecular velocity gradient (acoustic disturbance) associated with a density change induced by weak absorption of a 1.06 μm excitation pulse, causes molecular alignment through translational–rotational coupling. Using an optical heterodyne detection method, molecular orientational relaxation is monitored. An eightfold experimental cycle, analogous to phase cycles in NMR, is used to separate the DIHARD signal (density induced heterodyne amplified rotational dynamics) from optical Kerr effect (OKE) contributions and thermal lensing effects. Calculations combining the Navier–Stokes equation with translational–rotational coupling are presented that describe the nature of the method. The method is analyzed theoretically and demonstrated with experiments on supercooled salol (phenyl salicylate). DIHARD experiments on salol combined with heterodyne detected OKE experiments are used to examine long time scale orientational relaxation over a wide range of times and temperatures. While OKE experiments measure the time derivative of an orientational correlation function, it is shown that DIHARD directly measures the time dependence of an orientational correlation function. The experimental results are compared to those previously reported in the literature, which were obtained with other methods. © *1999 American Institute of Physics.* [S0021-9606(99)51929-6]

I. INTRODUCTION

In this paper a new method for the time domain measurement of orientational relaxation of molecules in viscous liquids is demonstrated experimentally and theoretically and applied to the study of the supercooled liquid salol (phenyl salicylate). The method, called density induced heterodyne amplified rotational dynamics (DIHARD) can induce an orientational anisotropy using a short pulse of light even when the time scale for orientational relaxation is very long.[1] The induced anisotropy is heterodyne detected as in a heterodyne detected optical Kerr effect experiment (HD-OKE). In contrast to an OKE experiment, the DIHARD experiment creates an orientational anisotropy mechanically, on a time scale that is unrelated to the time scale for orientational relaxation. While OKE experiments measure the time derivative of an orientational correlation function,[2] it is shown that DIHARD measures the time dependence of an orientational correlation function directly.

The OKE mechanism for inducing an anisotropy differs depending on whether the excitation pulse is short (large bandwidth) or long (small bandwidth).[3] For a short pulse, ~100 fs, stimulated Raman scattering excites an anisotropic orientational distribution of librations that add to the isotropic thermally excited librations. The librations damp and leave an ensemble average molecular orientation that is no longer isotropic. The residual anisotropy following librational damping decays by orientational relaxation, but there is little amplitude in very slow components. If the pulse is long, ~100 ps, the bandwidth is too narrow to excite librations by stimulated Raman scattering. An anisotropy develops because the **E** field skews the thermal orientational fluctuations of molecules in a liquid. Little amplitude develops in relaxation components that are much longer than the pulse duration.

In contrast to OKE experiments, DIHARD does not depend on stimulated Raman scattering or the intrinsic thermal motions of the sample to produce orientational anisotropy. Therefore, it is able to generate substantial amplitude in slowly decaying components of orientational relaxation. It is possible to study slow relaxation using the same short excitation pulses and almost the same HD-OKE experimental setups that are used to study fast orientational relaxation.

In a DIHARD experiment, a very small fraction of a short excitation pulse is absorbed by the sample, creating a small local temperature increase. The sudden heating launches an acoustic disturbance, which propagates radially outward from the heated spot at the velocity of sound. Once the acoustic disturbance has left the excitation spot, a small decrease in density remains. The spot of decreased density lasts for a time determined by the liquid's thermal conductivity and the spot size. This density change is well known in the context of thermal lensing experiments[4] and has been used to measure extremely weak absorptions.[5]

The density decrease results from a net outward flow of molecules from the heated region. The flow is accompanied by a spatial velocity gradient. A velocity gradient produces molecular orientational alignment of asymmetrical molecules.[6] This is, in essence, translational–rotational coupling. The resulting orientational anisotropy generates a birefringence, which can be heterodyne detected using a probe

a)Electronic mail: fayer@fayerlab.stanford.edu

beam in the same manner as heterodyne detection of orientational anisotropy induced by the OKE.[7] Creating an optical birefringence through a strain, such as the velocity gradient, has been observed in numerous other contexts, e.g., in flows of viscoelastic fluids,[8] in polymers,[7] in liquid crystals,[9] in glasses,[10] and in crystals.[11] While ultrasonic acoustic experiments have been used to obtain orientational relaxation parameters,[12] DIHARD is the first technique that uses the liquid state translational–rotational coupling effect to obtain direct time domain measurements, and the measurements can be made using heterodyne detection.

In the DIHARD experiment, the nature of the observed signal depends on the location of the probe beam relative to the excitation spot. If the probe is placed precisely in the center of the excitation spot, no signal is observed because the molecular alignment is radially symmetric (no orientational anisotropy). If the small probe spot is located within the excitation spot, but off center, the signal grows as the acoustic disturbances propagate out of the excitation spot leaving behind the nonpropagating density change. The signal then decays with the orientational relaxation dynamics of the sample. If the probe beam is placed well outside of the excitation spot, the signal grows and then dissipates as the acoustic disturbances pass through the probe spot. Outside the excitation spot, there is no long-lived orientational anisotropy because there is no long-lived density change. The long-lived orientational anisotropy that exists within the excitation spot makes DIHARD distinct from acoustic measurements.

With the probe located within the excitation spot but off center, a substantial long-lived DIHARD signal will be observed if the orientational relaxation time is slow compared to the time scale for the acoustic disturbance to propagate out of the excitation spot. This time scale is also the intrinsic response time of the technique since the signal builds up on this time scale. By making the excitation spot size small (20 μm), the time scale can be 10 ns. Thus, DIHARD is useful for studying relatively slow orientational relaxation. Transient grating OKE (TG-OKE) and HD-OKE experiments work well on femtosecond, picosecond, and nanosecond time scales.[13] Like OKE experiments, DIHARD is detected through contributions to the macroscopic anisotropic polarizability induced in the sample by the molecular alignment process. DIHARD is sensitive to contributions from both single particle and multiparticle polarizabilities.

Orientational relaxation of molecules has been studied extensively to obtain an understanding of dynamics in liquids. Many methods have been used, including NMR,[14] light scattering,[15] fluorescence depolarization,[15] dielectric spectroscopy,[16] and optical Kerr effect (OKE) experiments.[17] In supercooled liquids, the time scale on which rotational dynamics takes place can vary over many decades, even at a single temperature.[18] Only a few experimental techniques, such as dielectric spectroscopy[19] or dynamical light scattering,[20] exist which are, in principle, capable of covering the necessary time or frequency regimes. On very fast time scales, the OKE experiment is particularly useful. Using polarization selectivity in a transient grating OKE experiment, it is possible to eliminate the contribution of electronic polarization, which dominates the short time (the time scale of the pulse duration) signal.[21] The HD-OKE can provide very good signal-to-noise ratios at the polarization level, making it possible to directly measure the response function. However, as discussed above, OKE experiments have serious drawbacks for the examination of very slow responses in viscous liquids.

DIHARD combines smoothly with HD-OKE experiments, the latter being used at short times and the former being used at long times. After presenting the details of the DIHARD method, HD-OKE and DIHARD experiments are combined to examine orientational relaxation of salol from 290 to 240 K. The measurements cover a wide range of times, and they are compared to previous measurements using other techniques.

II. THEORY

The theoretical description of the DIHARD effect can roughly be divided into two parts. We first summarize the basic equations which describe the interactions between the laser radiation field and the hydrodynamic modes of an isotropic liquid.[22–25] The second part deals with the coupling of the relevant hydrodynamic modes to the molecular orientation.

Assuming a uniform density ρ_0 and temperature T_0, the continuity and Navier—Stokes equation

$$\left(-\frac{\partial^2}{\partial t^2}+\frac{C_v v^2}{C_p}\nabla^2+\frac{\eta}{\rho_0}\frac{\partial}{\partial t}\nabla^2\right)\rho_1+\frac{C_v v^2 \beta \rho_0}{C_p}\nabla^2 T_1 = \frac{\gamma^e}{2nc}\nabla^2 I \tag{1}$$

and the energy transport equation

$$\left(\rho_0 C_v \frac{\partial}{\partial t}-\lambda\nabla^2\right)T_1-\frac{(C_p-C_v)}{\beta}\frac{\partial \rho_1}{\partial t}=\alpha I \tag{2}$$

are sufficient to calculate the perturbations in density, ρ_1, and temperature, T_1, caused by picosecond pulsed laser excitation. C_p and C_v are the constant pressure and constant volume heat capacities; v is the acoustic velocity; η is the viscosity; β is the coefficient of thermal expansion; λ is the thermal conductivity; c is the vacuum velocity of light; n is the refractive index; γ^e is the electrostrictive coupling constant; and α is the optical absorption constant. For a Gaussian excitation beam profile $I=I_0\exp(-2r^2/r_b^2)$ with a beam diameter (twice the standard deviation of the intensity) r_b and negligible attenuation of the excitation laser light by the sample, Brueck *et al.*[23] and Heritier[24] have solved the above equations for short laser pulse duration $\Delta t \ll r_b/v$. They obtain the time-dependent density change

$$\rho_1(t)=-\frac{\epsilon\alpha\beta}{\pi C_p}A+\frac{\gamma^e}{2ncv^2}\left(\frac{C_p}{C_v}-1\right)\frac{\partial}{\partial t}A + \frac{\epsilon\alpha\beta}{\pi C_p}\left(\frac{1}{(2\pi)^{1/2}r_b v}\right)\frac{\partial}{\partial t}B-\frac{\gamma^e}{2ncv^2}\frac{\partial^2}{\partial t^2}B \tag{3a}$$

with

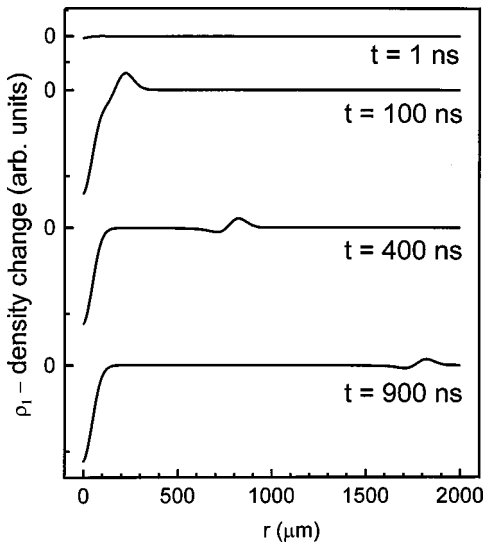

FIG. 1. Calculated density changes following weak absorption of light in a 100 μm spot as a function of distance at four different times. At very short times ($t=1$ ns) after the excitation pulse the density is essentially uniform. At longer times, an acoustic wave packet travels outward from the heated spot, leaving behind a region of reduced density. The calculations were performed using the parameter for a typical organic liquid (see the text).

$$A=\frac{\exp[-r_2/[(r_b^2/2)+(4\lambda t/\rho_0 C_p)]]}{(r_b^2/2)+(4\lambda t/\rho_0 C_p)}, \tag{3b}$$

$$B=\int_r^\infty\left\{\exp\left[-2\left(\frac{s-vt}{r_b}\right)\right]-\exp\left[-2\left(\frac{s+vt}{r_b}\right)\right]\right\}\times(s^2-r^2)^{-1/2}\,ds, \tag{3c}$$

where t is the time measured from the end of the laser pulse, and ϵ is the integrated pulse energy. The first two terms in Eq. (3a) describe the excitation of the diffusive mode while terms 3 and 4 describe the acoustic modes.

In Fig. 1, the density change, ρ_1, produced by weak absorption of a short laser pulse is plotted using parameters which are typical for liquids like salol ($v=2000$ ms^{-1}, $C_p=1465$ J kg^{-1} K^{-1}, $\lambda=1.27$ W m^{-1} K^{-1}, $\rho_0=838$ kg m^{-3}, $r_b=10^{-4}$ m). Since $\gamma^e=0$ is assumed, ϵ, α, and β can be set arbitrary, and C_v, n, and c are no longer necessary. Contributions from electrostriction have been neglected because experiments have shown that it is a much weaker effect than heating, even when the heating is produced by absorption of 1.06 μm by vibrational overtones.[26,27] At very short times after the laser pulse ($t=1$ ns), there is virtually no density change. The molecules have net velocity outward, but there is insufficient time for macroscopic displacement. By 100 ns, the acoustic disturbance can be seen to be leaving the initially heated spot, 100 μm in diameter in the calculations, leaving behind the density change. At 400 ns, the acoustic disturbance is well outside of the heated spot, and the density change remains. The lifetime of the remaining density change is determined by thermal diffusion. At 900 ns, the acoustic disturbance has continued to propagate. Because the time scale for thermal diffusion is very long, the density decrease in the initial spot is still virtually at its maximum value at 900 ns.

The equations used to perform the calculations in Fig. 1 were solved previously in the context of photoacoustic and photorefractive (thermal lensing) effects.[23,25] As will be shown below, while the local density change is responsible for thermal lensing,[13,28] it is also the basis of DIHARD because translation–rotational coupling produces molecular alignments.

The symmetry of the DIHARD problem allows it to be reduced to one dimension. For weak absorption, the pump laser beam passes through the sample with negligible attenuation. Heating and density changes are identical in all planes perpendicular to the pump beam propagation direction. Because the sample cell is thick (1 cm), boundary effects on the inner surfaces of the cell are neglected. Surface boundary effects should only be important when the sample thickness approaches the laser spot size. A flow gradient produces the molecular alignment. The intensity distribution of the pump laser beam, which is in the TEM_{00} mode, is a radially symmetric Gaussian. Therefore, the thermally induced density change and the net flows of molecules are radial symmetric as well. The flow gradient can be expressed in terms of the velocity gradient, which is connected to the density change via the linearized continuity equation[29]

$$\frac{\partial\rho}{\partial t}+\operatorname{div} w=0, \tag{4a}$$

which in our case can be reduced to

$$\frac{\partial\rho(r)}{\partial t}=-\frac{\partial w_r}{\partial r}, \tag{4b}$$

where w is the flow velocity and r is the distance from the center of the pump beam.

Molecular alignment caused by flow, stress, or strain is well known in the context of polymer processing,[7,30] where it can lead to unwanted optical properties of the materials. Flow birefringence, in which viscous liquids,[31] particles in a liquid,[32,33] or liquid crystals[34] are subjected to a shearing force causing birefringence has received a great deal of study. Depolarized light scattering experiments of anisotropic fluids have been interpreted in a similar manner using flow–rotational coupling.[6,35–38]

To describe the nature of the DIHARD experiment, an empirical equation for the translational–rotational coupling is sufficient. Assuming a velocity gradient in one direction, the coupling to the molecular orientation can be described by[6,31]

$$\frac{\partial S_{ik}}{\partial t}=-\frac{1}{\tau}S_{ik}+C\frac{\partial w_r}{\partial r}, \tag{5}$$

where S_{ik} denotes an anisotropy tensor ($i,k=1,2,3$) defining the average degree of orientation of the molecules in a liquid.[39] The coupling strength between the acoustic mode and reorientation is expressed by C. Once the forces causing the orientation cease, the anisotropy does not vanish immediately but decays away with a relaxation time τ. Equation (5) describes the orientational relaxation in terms of a single relaxation time, τ, i.e., an exponential decay of S_{ik}. This is sufficient for the development to illustrate the nature of the effect. In real liquids, a more complicated form of the orien-

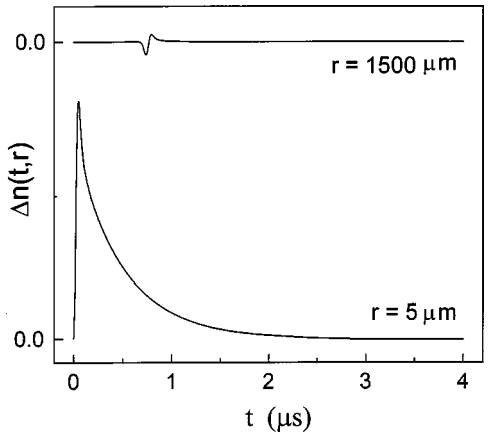

FIG. 2. Calculated induced birefringence (molecular alignment) using the same parameter as for Fig. 1. The molecular orientational relaxation time is $\tau=5\times10^{-7}$ s. In the upper trace, the probe is located well outside the pump spot at $r=1500$ μm. The passing acoustic wave lead to a temporary birefringence, which vanishes once the wave has passed by the probe spot. The lower trace is a calculation with the probe within the pump spot but slightly ($r=5\mu$m) off center. The thermally induced density gradient supports a long-lived molecular alignment, which decays with the molecular orientational relaxation time, τ.

tational relaxation will generally be required.[18] Due to the radial symmetry of the flow outward from the heated spot, the anisotropy averaged over the entire sample will be zero. However, in the experiment the probe is small and displaced from the pump spot. Therefore, a significant birefringence is detectable.

Using the same parameters as were used in the calculations presented in Fig. 1, we have calculated the induced anisotropy by solving Eq. (5) numerically with $\tau=5\times10^{-7}$ s. In Fig. 2, the resulting birefringence, $\Delta n\propto S_{ik}$, is plotted for two different probing positions. The probe beam is much smaller than the pump beam, which has a diameter of 100 μm. In the first case the probe beam is far outside the pumped spot ($r=1500\,\mu$m). The acoustic disturbance, traveling outward from the pump spot, causes molecular alignment, which vanishes after the wave has passed the probe position. This phenomenon is due to the rarefaction pulse which follows the compression pulse in a two-dimensional wave.[24] The time required for the signal to appear is determined by the velocity of sound and the distance of the probe from the pumped spot. In the second case, the probe spot is displaced from the center of the pump spot by 5 μm ($r=5\,\mu$m), but the probe spot is still within the pump spot. Molecular alignment, and therefore, Δn, is created as the acoustic disturbance leaves the pumped spot. However, because a density change remains in the pumped spot for a time determined by the rate of thermal diffusion, the molecular alignment persists for a time determined by the orientational relaxation time, τ. In the $r=5\mu$m curve in Fig. 2, there is a short time transient of ~100 ns produced by the acoustic disturbance leaving the initially heated spot. Following this, the curve decays exponentially with the decay time $\tau=5\times10^{-7}$ s.

If the probe is exactly centered on the pump spot, there is no birefringence, Δn, because the molecular alignment is radially symmetric with respect to the probe. Figure 3 displays calculations of the signal intensity as a function of the probe position relative to the pump, which is centered at 0 for two probe spot sizes. The calculations are performed for a time long compared to the time required for the acoustic disturbance to leave the pump spot. The Gaussian pump spot is 100 μm in diameter, and the Gaussian probe spots are 25 μm (curve 1) and 50 μm (curve 2) in diameter. The maximum signal intensity has been normalized. As can be seen in the calculation, when the probe is centered on the pump, there is no signal. A particular displacement from the pump spot center gives the maximum signal, and the location of the maximum depends on the relative pump–probe spot sizes.

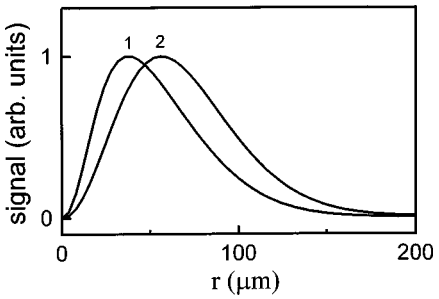

FIG. 3. The DIHARD signal intensity is calculated as a function of the probe position relative to the pump (100 μm in diameter), which is centered at 0 for two probe spot sizes—25 μm (curve 1) and 50 μm (curve 2). The calculations are performed for a time that is long compared to the time required for the acoustic disturbance to leave the pump spot. The maximum signal intensity is normalized. When the probe is centered on the pump, there is no signal. A particular displacement from the pump spot center gives the maximum signal, and the location of the maximum depends on the relative pump–probe spot sizes.

The DIHARD experiment can be used to study orientational relaxation on time scales long compared to the time required for the acoustic disturbance to leave the initially pumped spot if the probe is placed off-center but within the pump spot. DIHARD's usefulness occurs because the alignment is mechanical. The induced birefringence does not depend on thermal motions to align molecules with an electric field, as in the OKE. Thus, it is possible to obtain significant amplitude in slowly decaying modes even with an optical pulse that is very short compared to the time scales of slow relaxation. The excitation process that is responsible for DIHARD can also produce an OKE signal and a thermal lensing signal. As will be shown below, experimental methods have been developed to eliminate these other effects from the data to yield a clean DIHARD decay.

III. EXPERIMENTAL PROCEDURES

The setup of the DIHARD experiment is illustrated schematically in Fig. 4. A 100 ps duration 1.06 μm excitation pulse is produced by a mode-locked *Q*-switched cavity dumped Nd:YAG laser, which can deliver energies in excess of 1 mJ/pulse at repetition rates of 1 kHz or lower.[40] The excitation pulse is attenuated to produce ~50 μJ at the sample and has a 300 μm spot size. Higher intensities caused a variety of deleterious effects. The excitation pulses pass through a mechanical chopper that chops the pump beam at half the laser repetition rate. It then passes though a half wave plate and a polarizer set at 45°. The half wave plate,

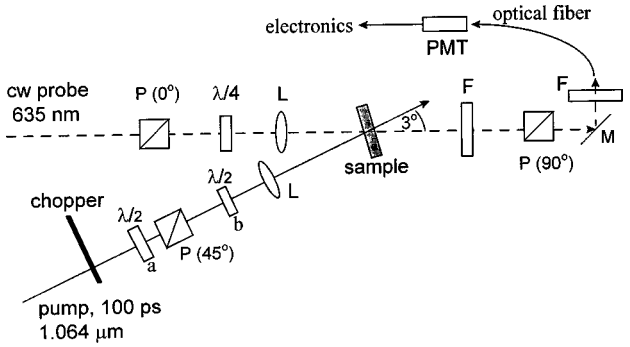

FIG. 4. Experimental setup for performing DIHARD and HD-OKE experiments and separating the various contributions to the signal (see the text). P: polarizer, L: lens, F: filter, M: mirror, PMT: photomultiplier tube, λ/2, λ/4: wave plates.

labeled (a) in Fig. 4, is used to attenuate the beam. The half wave plate, labeled (b) is on a motorized, computer controlled rotation stage, which permits the polarization of the IR pulses to be rotated 90°, from +45° to −45°. As discussed further below, this feature is essential for the experiments. By changing the polarization of the pump beam it is possible to separate the OKE and DIHARD signals.

In the OKE experiment, the strong field associated with the pump pulse induces an orientational anisotropy in the sample which depends on the polarization of the pump pulse. DIHARD is produced by a thermal effect caused by absorption of the pump pulse. Since the absorption is by randomly oriented molecules, the generation of the DIHARD signal is independent of the polarization of the pump beam. Both DIHARD and OKE produce birefringence in the sample. The birefringence is observed using heterodyne detection. Because of the heterodyne detection, rotating the polarization 90° of the pump pulse changes the sign of the HD-OKE signal while the thermally induced DIHARD signal is unaffected. Figure 5 illustrates the effect of rotating the polarization 90°. The data were taken on the pure liquid salol (phenyl salicylate) In Fig. 5(a), the sharp peak at $t \cong 0$ is produced by the HD-OKE, while the second, broader peak, is the DIHARD signal. As shown in Fig. 5(b), changing the polarization of the pump beam by 90° has inverted the HD-OKE signal but left the DIHARD signal unchanged. By taking two data sets with the polarizations differing by 90° and adding them, the HD-OKE can be eliminated. If the data sets are subtracted, DIHARD is eliminated.

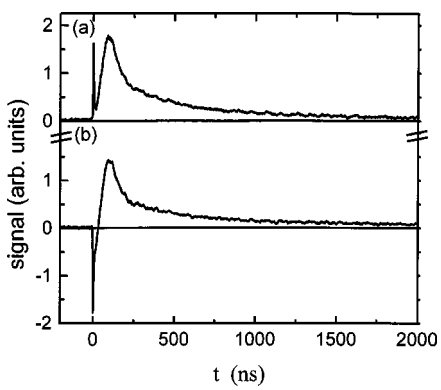

FIG. 5. Heterodyne detected birefringence in salol at 253.3 K after a 100 ps IR pump pulse. (a) The sharp peak at $t \cong 0$ is produced by the HD-OKE, while the second, broader peak, is the DIHARD signal. The DIHARD signal displays the long decay, which is the orientational relaxation. The HD-OKE signal is dominated by the electronic polarization and shows very little long decay components. (b) Changing the polarization of the pump beam by 90° has inverted the HD-OKE signal but left the DIHARD signal unchanged.

A cw laser diode with 10 mW of power at 635 nm is used as the probe laser beam in the heterodyne detection method. The heterodyne technique requires a local oscillator which is generated by a quarter wave plate (λ/4 in Fig. 4). The wave plate is rotated a small amount, θ, to produce a slightly elliptically polarized beam. The short axis component of the ellipse is the local oscillator. The λ/4 plate is mounted on a computer-controlled rotation state. Rotating the λ/4 plate from θ to $-\theta$ produces a phase shift of 180° in the local oscillator field. With heterodyne detection, the local oscillator, L, is large compared to the signal S. The measured intensity is $I = L^2 + 2LS + S^2$. The 180° phase shift, changes the sign of L, and inverts the sign of the DIHARD. Any thermal lensing contributions to the measurement, as well as possible S^2 contributions, are unaffected by the phase shift. Therefore, by taking data sets with the λ/4 plate at $\pm\theta$, and adding them, these unwanted contributions are eliminated.

The pump and the probe beam are crossed in the sample at an angle of roughly 3°. To control the overlap and the spot sizes of both beams, a charge-coupled device (CCD) is placed at the position of the sample. With the CCD, an accurate placement of the beams is possible, which is important as discussed above.

A fast photomultiplier tube (Hamamatsu R 5600-01) is used for detection. The phototube output is preamplified using a Stanford Research Systems SR 240 amplifier and then digitized by a fast EG&G transient digitizer (9846), which provides 2 ns time resolution. To reduce electrical noise pickup from the laser, the phototube is placed ~20 ft from the experiment, and the signal beam is passed through an optical fiber to bring it to the phototube. A mechanical chopper is used to block every other IR pulse to further reduce electrical noise that is correlated with the pump pulse.

Altogether, the chopper, the λ/2 plate, which rotates the pump polarization from +45° to −45°, and the λ/4 plate, which shifts the local oscillator phase by 180°, permit an eightfold cycle to be implemented. Table I describes the various combinations obtained in the cycle. Columns 2–4 define the state of each of the three devices that affect the signal. Under chopper, 1 and 0, mean the pump beam is passed and blocked, respectively. Under Φ_{pump}, the plus (+) and minus (−) mean the pump polarizations are +45° to −45°, respectively. Under Φ_{probe}, + and − mean the probe phase is 0 and 180°, respectively. Columns 5–7 show the signs of the different contributions OKE, DIHARD, and thermal lensing, respectively. Zero means no signal. Row 8 includes other electrical signals (noise), possible baseline zeroing errors, etc. The data acquisition procedures enabled all of the combinations in Table I to be acquired. To avoid problems of long term drifts, the various combinations were interspersed, with the wave plate settings being change on the order of every minute. The data were accumulated over pe-

TABLE I. Eight fold polarization cycle. Columns 2–4 are the input ''polarizations'' while rows 5–7 show the signs of the different contributions OKE, DIHARD, and thermal lensing, respectively. Row 8 includes all signal contributions, which are not due to the pump pulse, e.g., constant baseline shifts, etc.

No.	Chopper	Φ_{pump}	Φ_{probe}	OKE	DIHARD	Thermal lens	Other
P_1	1	+	+	+	-	+	+
P_2	0	+	+	0	0	0	-
P_3	1	-	+	-	-	+	+
P_4	0	-	+	0	0	0	-
P_5	1	+	-	-	+	+	+
P_6	0	+	-	0	0	0	-
P_7	1	-	-	+	+	+	+
P_8	0	-	-	0	0	0	-

riods of many minutes to many hours, depending on the signal-to-noise ratio of the measurement.

The different contributions permit the DIHARD signal (S_D) and the HD-OKE signal (S_O) to be independently obtained by properly adding and subtracting the cycle steps, P_i. Although it was not used in these experiments, the thermal lensing effect (TL) can also be obtained,

$$S_D = -P_1 + P_2 - P_3 + P_4 + P_5 - P_6 + P_7 - P_8, \quad (6)$$

$$S_O = P_1 - P_2 - P_3 + P_4 - P_5 + P_6 + P_7 - P_8, \quad (7)$$

$$\mathrm{TL} = P_1 - P_2 + P_3 - P_4 + P_5 - P_6 + P_7 - P_8. \quad (8)$$

In the temperature-dependent data presented below, DIHARD was used at low temperatures and for the long time component of the signal at high temperature. At the highest temperatures studied, the decays were fast and strong enough to use HD-OKE experiments. In all cases, the same excitation source was used. HD-OKE data taken for times >10 ns, were recorded as described above using the cycle sequence in Eq. (7). For times of 100 ps to 12 ns, the HD detected probe is a picked off piece of the excitation beam, doubled to 532 nm, and run down a computer-controlled delay line with 12 ns of delay.

The salol sample was obtained from Aldrich. The sample was purified by vacuum distillation into a 1 cm glass cell. Temperature stability of ± 0.1 K was maintained using a closed cycle helium refrigerator from Janis Technology.

IV. RESULTS AND DISCUSSION

In Figs. 1 and 2, calculations were presented that show the acoustic packet moving outward from the initially pumped spot. While Fig. 1 shows the density change, Fig. 2 is a calculation of the induced birefringence. As discussed in Sec. III, the heterodyne detected signal can be recorded in a manner that is exclusively sensitive to the birefringence, i.e., the molecular orientational anisotropy. Figure 6 displays time-dependent anisotropy data taken on salol at 257.2 K with the probe beam at two locations well outside the initially pumped spot. The relative locations of the pump and probe beams were determined with a CCD camera. Because the signal is heterodyne detected, either sign of the signal can be chosen. Here, the leading part of the acoustic disturbance (detected at short time) is positive. The calculations in Fig. 2 show that the absolute sign has the leading part negative. The time of the peak of the signal is plotted versus the relative location of the pump and probe beams for three locations in the inset. The slope of the line yields the velocity of sound. The velocity of sound was found to be 1880 m/s, which is in exact agreement with literature data.[41]

In Sec. III the eightfold cycle that can be used to separate different components of the signal was described. Equations (6)–(8) give the combination of cycle steps that permit each type of signal to be observed. Figure 7 demonstrates the extraction of each type of signal from measurements on supercooled salol at 250.4 K. The raw data are displayed in the upper part of Fig. 7 and the HD-OKE DIHARD, and thermal lensing signals are displayed at the bottom. In these experiments, the probe is located within the pump spot. At this temperature, the HD-OKE signal is still observable but significantly smaller than the DIHARD signal. At lower temperatures, the long time HD-OKE signal is undetectable in contrast to the DIHARD signal, which remains strong.

The experiments were conducted on salol since it is a fragile glass forming liquids which is studied extensively in the literature.[18] Performing DIHARD experiments on salol makes it possible to compare the DIHARD data to that taken with different experimental techniques, and additional infor-

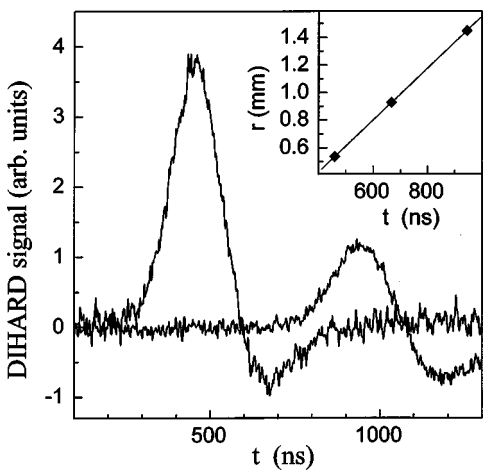

FIG. 6. DIHARD signal in supercooled salol (257.2 K) detected at two locations well outside the initially pumped spot. The relative locations of the pump and probe beams were determined with a CCD camera. The signal reflects the birefringence produced as the acoustic wave packet passes through the probed region. In the inset the time of the peak of the signal is plotted vs the relative location of the pump and probe beams for three locations. The slope of the line yields the velocity of sound $v = 1880$ m/s, which is in exact agreement with literature data (Ref. 41).

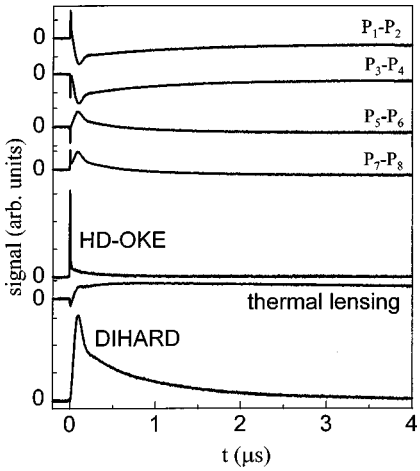

FIG. 7. Data from supercooled salol at 250.4 K using the eightfold cycle described in the text. By combining various parts of the cycle it is possible to cleanly extract each contribution to the signal [see Eqs. (6)–(8) and Table I]. The raw data P_1-P_2, P_3-P_4, P_5-P_6, P_7-P_8 as well as the extracted OKE, DIHARD and thermal lensing signals are plotted. Note the very low amplitude of the long-lived component of the HD-OKE data relative to the DIHARD data.

mation on details of molecular reorientation might be obtained.[42] Because it is highly polarizable, salol is an excellent candidate for application of optical methods like dynamical light scattering[43] or OKE experiments.[44] The detection of the DIHARD signal is identical to that of the HD-OKE signal, and, therefore, requires anisotropic molecular polarizability. Also, salol has a somewhat stronger absorption and an increased DIHARD signal compared to other glass formers like *o*-terphenyl or toluene, possibly because of the contribution of overtone absorption by the OH stretch at 1.06 μm.

Relaxation data on salol were taken in the temperature range 240.7–290.1 K, which is above the calorimetric glass transition temperature, $T_g = 218$ K.[44] Since in this regime the structural relaxation times vary over almost 5 decades, OKE and DIHARD data were combined. For the OKE data, the delay line was used for $t < 12$ ns, while at longer times the OKE signal was extracted from the cw probe signal. For $t \geqslant 300$ ns, the DIHARD signal was obtained from the same cw probe data sets, as discussed in conjunction with Fig. 7.

Particular care has to be taken in the evaluation of the data. Since the IR pump pulses were always short compared to the time scales of molecular reorientation, the HD-OKE experiment measures the impulse response function

$$S(t) \propto \frac{\partial}{\partial t} C^{\epsilon\epsilon}(t), \tag{9}$$

where $C^{\epsilon\epsilon}(t)$ is the dielectric constant time correlation function.[2] In the OKE, the molecular alignment is achieved by an optical field which is short compared to the time scale of the dynamics being probed. The degree of alignment depends on the time scale of the molecular dynamics. The applied electric field skews the normal thermal orientation motions causing an orientational anisotropy to develop. Because salol and other molecules studied with the OKE have anisotropic polarizabilities, orientational relaxation is directly related to $C^{\epsilon\epsilon}(t)$. To illustrate the difference between the observables in the HD-OKE and DIHARD experiments, consider orientational relaxation that gives rise to a biexponential for $C^{\epsilon\epsilon}(t)$, i.e.,

$$C^{\epsilon\epsilon}(t) = \alpha_1 e^{-k_1 t} + \alpha_2 e^{-k_2 t}, \tag{10}$$

where $k_1 > k_2$, and α_1 and α_2 are amplitude factors. From Eq. (9), the HD-OKE signal is

$$S(t) = \alpha_1 k_1 e^{-k_1 t} + \alpha_2 k_2 e^{-k_2 t}. \tag{11}$$

In the HD-OKE signal, the amplitude of each term is multiplied by the decay constant k_i. Since intrinsic thermal motions are required to build up the anisotropy, the orientational component with faster dynamics undergoes more motion that is skewed by the applied $\vec{E}$ field. Therefore, for a short excitation pulse, the faster dynamical component builds up more amplitude. This is reflected in Eq. (11), the derivative of the correlation function. In the limit that an $\vec{E}$ field is applied for a time long compared to all of the dynamics, the amplitude of each decay component is independent of the applied $\vec{E}$ field. The buildup of the anisotropy is saturated. The amplitude of each decay component depends on the magnitude of the field and molecular polarizability anisotropy, but not the decay constants. Following the application of a long optical field, if the field is suddenly turned off, the resulting decay reflects the correlation function, $C^{\epsilon\epsilon}(t)$, not its time derivative. These considerations apply for any form of $C^{\epsilon\epsilon}(t)$, not just the simple biexponential used as an illustration.

The induction of the DIHARD signal also occurs on a time scale which is short compared to the structural relaxation time. However, the mechanism of molecular alignment is significantly different. In DIHARD, the molecular alignment is attained through translational–rotational coupling, which does not depend on the intrinsic thermal motions of the molecules. Therefore, the development of orientational anisotropy does not depend on the orientational relaxation times of the system if they are long compared to the duration of the velocity gradient that induces the molecular alignment. It has been shown that the translational–rotational coupling is virtually temperature independent.[37,45] The degree of alignment does depend on how large the velocity gradient is and how long it is applied. However, the intrinsic relaxation dynamics of the system do not come into play in determining the degree to which the relaxation components develop anisotropy. In this sense, it is as if the alignment is saturated, which corresponds to an infinity long pump pulse in the OKE experiment. Therefore, it is proposed that DIHARD measures a correlation function, $C_D^{\epsilon\epsilon}(t)$, instead of its derivative.

In the HD-OKE experiment, the alignment inducing force arises through coupling of the applied $\vec{E}$ field to the polarizibility tensor of the molecules. In DIHARD, mechanical force couples to geometric parameters of the molecular shape, producing the molecular alignment. Since in both experiments, the decay of the polarizibility anisotropy is monitored in an identical manner, in the following it is assumed that the two correlation functions are approximately equal,

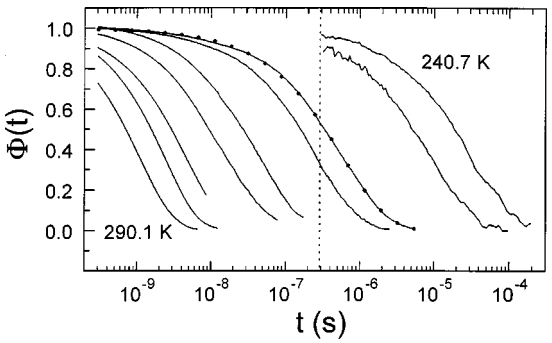

FIG. 8. The relaxation decays $\phi(t)$ [Eqs. (12) and (13)] composed of HD-OKE and DIHARD data are plotted for nine temperatures: 240.7, 243.6, 250.4, 253.3, 261.4, 266.2, 271.0, 280.6, and 290.1 K. The dashed line indicates the transition from HD-OKE to the DIHARD signal. Two of the curves are combined HD-OKE and DIHARD data. In the data analysis (Fig. 9), the curves are fit to a stretched exponential [Eq. (13)]. The points plotted on the 250.4 K curve show the quality of the fit to the data.

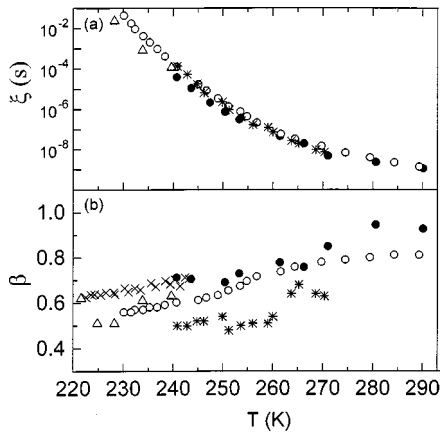

FIG. 9. (a) The integral of the normalized data, ξ (frequently referred to as the mean correlation time), and (b) the stretching parameters β obtained from the data in Fig. 8 by fitting to a stretched exponential function (see the text) as a function of temperature. closed circles are the data from these experiments. For comparison, salol data obtained by dynamic light scattering—Ref. 46 (open triangles), dielectric relaxation—Ref. 47 (open circles), specific heat spectroscopy—Ref. 47 (crosses), and thermal grating technique—Ref. 41 (asterisks), are also plotted.

$C^{\epsilon\epsilon}(t) \approx C_D^{\epsilon\epsilon}(t)$. Thus, DIHARD measures basically the same correlation function as dynamic light scattering (DLS). In DLS, fluctuating forces produce anisotropic deviations from an isotropic liquid. The anisotropy is detected through the coupling of the molecular anisotropic polarizability to light. In DIHARD, an applied force (velocity gradient) produces anisotropy, which is detected through the coupling of the molecular anisotropic polarizability to light.

In Fig. 8 the resulting relaxation decays, $\phi(t)$, are plotted for the different temperatures. Since the HD-OKE measures the time derivative of the correlation function and DIHARD measures the correlation function directly, the data were made consistent by integrating the HD-OKE data, i.e.,

$$\phi(t) = \begin{cases} a_1 \int_0^t \frac{\partial}{\partial t'} C^{\epsilon\epsilon}(t')dt', & t < 33\ \text{ns} \\ a_2 C_D^{\epsilon\epsilon}(t), & t \geqslant 300\ \text{ns} \end{cases}, \tag{12}$$

where a_1 and a_2 denote constants which were adjusted to combine and normalize the data sets. The dashed line indicates the transition from OKE to DIHARD signal. Two of the data sets are composed of both HD-OKE and DIHARD data. The data were taken at the same time; therefore, there is no temperature difference for the two measurements. To combine the sets, the HD-OKE data were integrated and the amplitude factors were adjusted to account for differences in the signal strengths and the integration. The two types of data combine flawlessly. The fact that the data sets can be combined in this manner supports the idea that $C^{\epsilon\epsilon}(t) \approx C_D^{\epsilon\epsilon}(t)$.

To compare our results with previously reported data on salol, we followed the prevalent approach, which is to fit the data to a stretched exponential function,

$$\phi(t) = \alpha e^{-(t/\tau)^{\beta}}. \tag{13}$$

α is an amplitude factor. β is the ''stretching'' parameter. All of the data sets in Fig. 8 fit exceedingly well to a stretched exponential. One of the sets is shown with the corresponding fit as dots on top of the data. If an actual fit line is put through the data, the data are totally obscured. It is common to integrate the normalized data to obtain a measure of the decay which is independent of the functional form of the decay curve. For a stretched exponential, the integral, $\xi = \tau\beta^{-1}\Gamma(\beta^{-1})$, where Γ is the standard gamma function. ξ and β are plotted in Fig. 9 together with data from dynamic light scattering,[46] dielectric relaxation,[47] specific heat spectroscopy,[47] and thermal grating technique.[41] We find that the combined HD-OKE and DIHARD data agree reasonably well with the published data on the time scale ξ and the stretching parameter β. In the frequency domain measurements, e.g., dielectric relaxation and specific heat spectroscopy, the data were fit to the Fourier transform of a stretched exponential. In some cases, the shape of the data is not in good accord with the Fourier transformed stretched exponential. In the dielectric relaxation measurements, β was extracted using a procedure that assumes that the data are the Fourier transform of a stretched exponential. Therefore some deviations from the different experiments are expected.

However, significant deviations are seen in comparing the present OKE/DIHARD data to the thermal grating results,[41] although the grating experiment[26,41,48,49] bears some relationship to DIHARD. In thermal grating experiments, two short laser pulses are crossed within a sample to produce a combined acoustic and density grading via optical absorption.[27] The time evolution of the grating is monitored via a probe beam which diffracts off of the grating. The grating signal is generated by any physical effect that changes the samples index of refraction. The time dependencies of the longitudinal acoustic waves and thermal diffusion depend on the grating wave vector. The component of the signal that is wave vector independent is assigned to the structural relaxation process[48] also referred to as the Mountain mode.[15,50,51] The physical origin for the Mountain mode is not well understood. It is described as the slow structural response of a system to local changes in density and temperature. However, no satisfactory description exists for the structural relaxation.[52]

In analysis of the thermal grating experiments, two con-

siderations might alter the values of the β parameters extracted from the data. Decomposition of the thermal grating experiments used a stretched exponential fitting function to give the Mountain mode parameters.[41] Since the thermal grating experiment uses a short driving pulse, the investigators state that the experiment measures the impulse response function. If this is the case, the data should be fit to the derivative of a stretched exponential, rather than a stretched exponential if the thermal grating data are to be compared in a consistent manner with other data taken on the same system. Fitting the data to the derivative of a stretched exponential could result in a significant change in the stretching parameters β. In addition, no consideration of orientational effects was included in the data analysis. It is well established that the grating configuration employed will produce a transient grating optical Kerr effect (TG-OKE) signal which can be disguised by the acoustic and thermal gratings.[53] The TG-OKE signal comes from the contribution of orientational anisotropy to the grating's peak-null difference in the index of refraction. This technique has been used extensively to study orientational relaxation in pure liquids.[54–56] In addition, the thermal grating should produce molecular alignment in a manner analogous to the DIHARD experiment described here, since the density gradient remains on the time scale of the relevant portion of the data. Such molecular alignments will contribute to the signal just as OKE alignment gives rise to the TG-OKE signal.

In the experiment discussed in this paper, both changes in density and birefringence are recorded. The thermal contributions as well as the acoustic waves are common features in the DIHARD and the thermal grating experiments. Because DIHARD detects the induced birefringence, the nature of the motions being examined by the measurement is well defined.

As mentioned above, in a transient grating experiment translational rotational coupling can occur in a manner that is similar to that described for the DIHARD experiment. Birefringence induced as in DIHARD has not been considered in the literature in connection with grating experiments, although it might contribute to the overall signal in TG-OKE experiments as well as in thermal grating experiments. With the appropriate set of polarizations, it should be possible to separate the different contributions to the grating signal. We therefore propose a new experiment, in which both molecular reorientation and structural relaxation can be measured in the same experiment. This is interesting, especially in the context of supercooled liquids, since the origin of the structural relaxation is not well understood.[18] It should be possible to independently determine the orientational relaxation time and the density (structural) relaxation time in a sample under identical experimental conditions.

As in the DIHARD setup described in this work, the proper selection of the polarizations for pump and probe beams is essential in the proposed grating experiments. In a grating experiment, the four polarizations of the two pump pulses, the probe pulse, and the signal can be independently set. This polarizations (pump, pump, probe, signal) are $(\phi_1/\phi_2/\phi_3/\phi_4)$.[57] It has been shown[57] that polarization selection permits separation of contribution of different physical processes to the signal if they are characterized by different symmetries of the nonlinear susceptibility tensor $\chi^{(3)}$.

Assuming that only nuclear OKE (orientational), DIHARD, and density effects (e.g., Mountain mode) contribute to the overall signal in a grating experiment, the general approach is to find polarizations $(0°/\alpha/\gamma/\beta)$ which eliminate two of the three contributions. Since the symmetries of nuclear OKE $\chi^{(3)}$ and isotropic local density change $\chi^{(3)}$ are known,[57] the pure DIHARD-like signal can be obtained by choosing $\beta=\gamma+90°$ and $\sin(2\gamma)=-\tan(\alpha)$. Assuming that the elements of the DIHARD $\chi^{(3)}$ are $\chi^{(3)}_{1111}=-2\chi^{(3)}_{1122}$ as for the nuclear OKE but $\chi^{(3)}_{1212}=0$ (this excitation combination will not produce a DIHARD-like grating signal), the maximum DIHARD signal is obtained at $(0°/45°/-45°/45°)$. Then the pure signal arising from isotropic density changes can be isolated by choosing $(0°/0°/54.7°/54.7°)$. Thus, the polarization selectivity afforded in a grating experiment should make it possible to determine if orientational relaxation and structural relaxation occur with the same or different time dependencies.

V. CONCLUDING REMARKS

In this paper, DIHARD, a new time domain technique for studying molecular rotational dynamics in viscous liquids, was described and used to study the pure liquid salol. DIHARD is useful for the observation of slow orientational relaxation. Pulsed laser excitation OKE experiments are poor for generating significant amplitude in the very slow components of orientational relaxation. The DIHARD signal is detected in a manner which is identical to an HD-OKE experiment. The signal in both experiments depends on inducing an orientational anisotropy and observing the orientational anisotropy through the molecular anisotropic polarizability. However, in the DIHARD experiment, the anisotropy is induced mechanically. The mechanism depends on very weak absorption by the sample, as in a thermal lensing experiment. The absorption leads to molecular displacements, and, through translational–rotational coupling, orientational alignment. However, unlike a pulsed OKE experiment, which measures the impulse response (the time derivative of the dielectric correlation function), it was argued that DIHARD measures directly the correlation function.

Detailed calculations for a simple relaxation model were presented which show the spatial and time dependence of the generating mechanism and the signal. Experiments on supercooled salol demonstrate the nature of the new method. To enhance the signal, an eightfold phase/polarization/amplitude cycle, analogous to phase cycles in NMR, which permits the DIHARD signal to be separated from optical Kerr effect contributions and thermal lensing effects, was introduced. The experiments combined HD-OKE measurements with DIHARD measurements to examine orientational relaxation over a wide range of times and temperatures. It was demonstrated that HD-OKE and DIHARD data can be smoothly merged to form an extended data set. The temperature-dependent dynamics measured with the combined HD-OKE/DIHARD experiments are in good agreement with reported measurements made with other methods.

In the experiments presented above, very weak overtone absorption by the bulk liquid of 1.06 μm light was used to produce the local heating responsible for the DIHARD signal. Another possibility is to electronically excite a very low concentration solute, such as malachite green, which undergoes rapid radiationless relaxation. If the solute is in sufficiently low concentration, the signal will come from the bulk liquid, which will not be perturbed by the low concentration solute. It should also be possible to use two photon electronic absorption, if it is followed by rapid radiationless relaxation, to produce the necessary local heating. It may be possible to align large molecules, such as DNA, which are difficult to align with the OKE. Small solvent molecules will relax much faster than the macromolecules, so that the slow dynamics of the large molecules may be observable.

We have made measurements in a number of different liquids over a wide range of temperatures. Unlike HD-OKE experiments, we observed that the strength of the signal was almost temperature independent. It was possible to observe strong signals just above the glass transition. By making the excitation spot small, it should be possible to improve the time resolution to <10 ns. The longest time scale is restricted by thermal diffusion out of the initial heat spot. However, if the excitation spot size is increased, the rise time of the signal increases linearly with the spot size, but the time scale for thermal diffusion increases as the square of the spot size. Therefore, exceedingly slow orientational relaxation can be measured in the time domain using a large excitation spot size.

ACKNOWLEDGMENTS

We would like to thank Professor H. C. Andersen, Department of Chemistry, Stanford University for informative conversations pertaining to this work. This work was supported by the National Science Foundation (DMR-9610326). G.H. would like to thank the Humboldt Foundation for partial support.

[1] R. S. Francis, G. Hinze, and M. D. Fayer, Chem. Phys. Lett. **304**, 28 (1999).
[2] Y. Yan and K. A. Nelson, J. Chem. Phys. **87**, 6257 (1987).
[3] S. Palese, L. Schilling, R. J.. Dwayne Miller, P. R. Staver, and W. T. Lotshaw, J. Phys. Chem. **98**, 6308 (1994).
[4] J. B. Thone and D. R. Bobbitt, Appl. Spectrosc. **47**, 360 (1993).
[5] S. E. Bialkowski, *Photothermal Spectroscopy Methods for Chemical Analysis* (Wiley, New York, 1996).
[6] D. Kivelson, T. Keyes, and J. Champion, Mol. Phys. **31**, 221 (1976).
[7] T. Inoue, H. Matsui, S. Murakami, S. Kohjiya, and K. Osaki, Polymer **38**, 1215 (1997).
[8] T. Konig and H. Buggisch, Rheol. Acta **37**, 182 (1998).
[9] I. C. Khoo, R. G. Lindquist, R. R. Michael, R. J. Mansfield, and P. LoPresti, J. Appl. Phys. **69**, 3853 (1991).
[10] Y. N. K. Ichinose, JSME Int. J. **38**, 500 (1995).
[11] K. Ravi-Chandar, B. Adamson, J. Lazo, and J. P. Dempsey, Appl. Phys. Lett. **64**, 1183 (1994).
[12] H. D. Ouyang, R. A. Macphail, and D. Kivelson, Phys. Rev. A **33**, 611 (1986).
[13] H. M. Chen, Opt. Laser Technol. **28**, 615 (1996).
[14] H. W. Spiess, NMR **15**, 55 (1978).
[15] B. J. Berne and R. Pecora, *Dynamic Light Scattering* (Krieger, Malabar, FL, 1990).
[16] C. J. F. Boettcher and P. Bordewijk, *Theory of Electric Polarization* (Elsevier, Amsterdam, 1978).
[17] S. Mukamel, *Principles of Nonlinear Optical Spectroscopy* (Oxford University Press, New York, 1995).
[18] See the collection of papers in, *Supercooled Liquids, Advances and Novel Applications* (American Chemical Society, Orlando, FL, 1997), Vol. 676.
[19] P. Lunkenheimer, A. Pimenov, B. Schiener, R. Böhmer, and A. Loidl, Europhys. Lett. **33**, 611 (1995).
[20] R. Bergmann, L. Börjesson, L. M. Torell, and A. Fontana, Phys. Rev. B **56**, 11619 (1997).
[21] F. W. Deeg, J. J. Stankus, S. R. Greenfield, V. J. Newell, and M. D. Fayer, J. Chem. Phys. **90**, 6893 (1989).
[22] P. R. Longaker and M. M. Litvak, J. Appl. Phys. **40**, 4033 (1969).
[23] S. R. J. Brueck, H. Kildal, and L. J. Belanger, Opt. Commun. **34**, 199 (1980).
[24] J. M. Heritier, Opt. Commun. **44**, 267 (1983).
[25] M. Terazima and N. Hirota, J. Chem. Phys. **100**, 2481 (1994).
[26] R. J. D. Miller, R. Casalegno, K. A. Nelson, and M. D. Fayer, Chem. Phys. **72**, 371 (1982).
[27] K. A. Nelson, R. J. D. Miller, D. R. Lutz, and M. D. Fayer, J. Appl. Phys. **53**, 1144 (1982).
[28] M. Terazima, Chem. Phys. Lett. **230**, 87 (1994).
[29] K. F. Herzfeld and T. A. Litowitz, *Absorption and Dispersion of Ultrasonic Waves* (Academic Press, New York, 1959), Vol. 7.
[30] V. I. Brizitsky, G. V. Vinogradov, A. I. Isayev, and Y. Y. Podolsky, J. Appl. Polym. Sci. **22**, 751 (1978).
[31] N. C. Hilyard and H. G. Jerrard, J. Appl. Phys. **33**, 3470 (1962).
[32] F. J. Burger and K. Söllner, Faraday Soc. Trans. **32**, 1598 (1936).
[33] T. Yasunaga, N. Tatsumoto, and H. Inoue, J. Colloid Interface Sci. **29**, 178 (1969).
[34] S. Koda, T. Koyama, Y. Ennomoto, and H. Nomura, Jpn. J. Appl. Phys., Part 1 **S31**, 51 (1992).
[35] T. Keyes and D. Kivelson, J. Chem. Phys. **54**, 1786 (1971).
[36] D. Kivelson and P. A. Madden, Annu. Rev. Phys. Chem. **31**, 523 (1980).
[37] D. F. Calef and P. G. Wolynes, J. Chem. Phys. **72**, 535 (1980).
[38] W. T. Grubbs and R. A. MacPhail, J. Chem. Phys. **97**, 8906 (1992).
[39] J. Frenkel, *Kinetic Theory of Liquids* (Clarendon, Oxford, 1946).
[40] V. J. Newell, F. W. Deeg, S. R. Greenfield, and M. D. Fayer, J. Opt. Soc. Am. B **6**, 257 (1989).
[41] Y. Yang and K. A. Nelson, J. Chem. Phys. **103**, 7732 (1995).
[42] G. Diezemann, H. Sillescu, G. Hinze, and R. Böhmer, Phys. Rev. E **57**, 4398 (1998).
[43] G. Li, W. M. Du, A. Sakai, and H. Z. Cummins, Phys. Rev. A **46**, 3343 (1992).
[44] R. Torre, P. Bartolini, and R. M. Pick, Phys. Rev. E **57**, 1912 (1998).
[45] D. Kivelson and R. Hallem, Mol. Phys. **38**, 1411 (1979).
[46] D. L. Sidebottom and C. M. Sorensen, Phys. Rev. B **40**, 461 (1989).
[47] P. K. Dixon, Phys. Rev. B **42**, 8179 (1990).
[48] Y. Yang and K. A. Nelson, J. Chem. Phys. **103**, 7722 (1995).
[49] W. Köhler, G. Fytas, W. Steffen, and L. Reinhardt, J. Chem. Phys. **104**, 248 (1996).
[50] R. D. Mountain, J. Res. Natl. Bur. Stand., Sect. A **70**, 207 (1966).
[51] R. D. Mountain, J. Res. Natl. Bur. Stand., Sect. A **72**, 95 (1968).
[52] J. P. Boon and S. Yip, *Molecular Hydrodynamics* (McGraw–Hill, New York, 1980).
[53] G. Eyring and M. D. Fayer, J. Chem. Phys. **81**, 4314 (1984).
[54] A. Sengupta, M. Terazima, and M. D. Fayer, J. Phys. Chem. **96**, 8619 (1992).
[55] S. R. Greenfield, A. Sengupta, J. J. Stankus, M. Terazima, and M. D. Fayer, J. Phys. Chem. **98**, 313 (1994).
[56] J. J. Stankus, R. Torre, and M. D. Fayer, J. Phys. Chem. **97**, 9478 (1993).
[57] F. W. Deeg and M. D. Fayer, J. Chem. Phys. **91**, 2269 (1989).